Optical Engineering

SPIEDigitalLibrary.org/oe

Polarization and modal filters based on W-fibers Panda for fiber-optic gyroscopes and high-power fiber lasers

Alexander. M. Kurbatov
Roman. A. Kurbatov

SPIE

Polarization and modal filters based on W-fibers Panda for fiber-optic gyroscopes and high-power fiber lasers

Alexander. M. Kurbatov
Roman. A. Kurbatov
Kuznetsov Research Institute for Applied Mechanics
Department of Center for Terrestrial Space Infrastructure Objects Exploiting
Aviamotornaya Street, 55
Moscow 111123, Russia
E-mail: romuald75@mail.ru

Abstract. Polarizing Panda-type W-fibers, practical realizations are presented for fiber-optic gyroscope (FOG) sensing coil (500-m length, 8-μm fundamental mode field diameter) and for polarization/modal filtering at the FOG loop interferometer input (~1-*m* length, 10-μm fundamental mode field diameter). Using these fibers, two different mathematical models for light propagation are tested and applied for further dichroism spectral band spreading of polarizing W-fibers with fundamental mode field diameter (MFD) of 6 to 10 μm for FOG coil and at least with MFD = 8 to 10 μm for input filtering in loop interferometer. Also, some fibers with large MFD are considered, which may be useful for high-power fiber lasers, requiring the low nonlinear effects. One is a practically realized single-mode 200-m W-fiber Panda with dichroism and MFD = 12.4 μm at 1.06 μm, which is bend resistant for 60-mm diameters. For further MFD increase a straight 100-mm length modal and polarization filters are suggested with MFD = 30 to 70 μm at 1.06 μm, based on a pure silica core fiber, narrow/shallow fluorine cladding, and stress-applying parts. The latter are used for core refractive index regulation by birefringence (W-profile forming), which is more precise than with core germanium doping.
[DOI: 10.1117/1.OE.52.3.035006]

Subject terms: polarizing fibers; W-profile; Panda fibers; fiber loop interferometer.

Paper 121464 received Oct. 7, 2012; revised manuscript received Feb. 25, 2013; accepted for publication Feb. 25, 2013; published online Mar. 13, 2013.

1 Introduction

In single-mode (SM) fibers there are two mutually orthogonal fundamental polarization modes (*x*- and *y*-modes). Due to their cross-talk, total polarization will not be stable along the fiber even if only one of these modes excited at fiber input. However, a stable polarization is required in fiber communication lines[1] and fiber sensors.[2] It also will improve the high-power fiber lasers' performance.[3] Thus fibers are necessary, polarizing (PZ) at least within a certain spectral range (window). For this dichroism window, we assume that within it, *x*-mode loss does not exceed 0.1 dB and *y*-mode loss is above 30 dB on a fiber whole length (10 dB for higher-order *x*-mode and fundamental *y*-mode losses in high-power fiber laser modal and polarization filters).

In Sec. 2, we present a brief overview of polarization errors in Sagnac fiber loop interferometer (FLI), validating the necessity in different length PZ-fibers from 1 to 1000 m (for lasers this validating could be found in Ref. 3). In Sec. 3, we describe refractive index W-profile as a basis for a wide class of PZ-fibers and known from literature some PZ-fibers' realizations. In Sec. 4, we describe two mathematical models for such fibers' analysis. Section 5 describes a 500-m sample of Panda PZ-fiber, a prototype of PZ-fiber for FOG sensing coil, measures for further performance improvement of this kind of fiber, and an example of calculated W-profiles for coil PZ-fibers with different MFD from 6 to 10 μm. Section 6, in the same way, describes a short (~1 m) PZ-fibers Panda with calculated W-profiles examples with MFD from 8 to 10 μm. Finally, in Sec. 7, we describe some polarization and modal filters with raised and large MFD, which could be used in high-power fiber lasers.

2 Polarization Errors in Fiber Loop Interferometer

In FLI, which is, for example, a part of FOG, one fundamental accuracy limit is polarization nonreciprocity (PNR). It is caused by parasitic interference of *x*- and *y*-modes, passed through FLI with different velocities, when their small parts may be converted to another polarization state due to polarization mode coupling (PMC).

A well-known FLI minimal configuration[2] uses an input polarizer with amplitude extinction ratio $\varepsilon \ll 1$ to suppress *y* mode. First,[2] it was set $\varepsilon = 0$ (zero PNR), but for $\varepsilon \neq 0$ an extremely severe limitation of $\varepsilon^2 \sim 120$ dB was yielded.[4] However, then in it was shown in Refs. 5 and 6 that high birefringent (hi-bi) fiber coil together with broadband source strongly suppress PNR, so $\varepsilon^2 \sim 50$ dB is enough.[7]

Further, a total PNR is divided into three parts[8] $\psi_{1,2,3}$ in accordance with light Stokes parameters $s_{1,2,3}$, so $\psi_1 \sim \varepsilon^2$ (intensity PNR) and $\psi_{2,3} \sim \varepsilon$ (amplitude PNR's). That is to our knowledge a first PNR analytical treatment based on a distributed stochastic PMC model in coil fiber, along with its optical axes misalignment relative to the polarizer axes. In the absence of this misalignment one may write[8]

$$\psi_1 \sim s_1 \varepsilon^2 h \sqrt{L_\gamma L}, \qquad \psi_{2,3} \sim s_{2,3} \varepsilon \sqrt{h L_\gamma}, \tag{1}$$

where L_γ is depolarization length, L is fiber length ($L_y \ll L$), h is fiber h-parameter. Later, a numerical model was suggested for stochastic PMC,[9] which is universal for either hi- or lo-bi fibers. It treats the fiber as a sequence of short fiber sections with random lengths (on average 25 mm)

and random twists. For minimal FLI with hi-bi coil it agrees very well with Eq. (1).

Generally Eq. (1) yields $\psi_{2,3} \gg \psi_1$, so errors $\psi_{2,3}$ suppression, even with ψ_1 left unchanged, already means PNR large suppression. Moreover, although $\psi_1 \sim \varepsilon^2$, it could be effectively suppressed by FLI polarizer. For this purpose, several FLI schemes were suggested using an additional hi-bi optical element before or after the polarizer[10] for input x- and y-waves total decoherence, which should lead to $\psi_{2,3} = 0$. We further assume that it is hi-bi input fiber before the polarizer, although it also could be a proton-exchanged input waveguide of integrated optic chip (IOC).

However in Ref. 10, a high-order PMC is not considered in coil fiber. There is no need to do this for minimal FLI, but with input hi-bi fiber there will be small residual PNRs due to high-order PMC, which may set a new limitation on $\psi_{2,3}$ suppression.[11] Thus it can still be $\psi_{2,3} \gg \psi_1$. Of course, when $B_{\text{in}}L_{\text{in}} > BL$ (B_{in} and L_{in} are input fiber birefringence and length. B and L are the same for coil fiber.), then $\psi_{2,3}$ are fully suppressed. But this means $L_{\text{in}} \sim L$, which is undesirable constructively Also, this leads to PNR suppression limitations due to PMC in the long input fiber itself. So we take $L_{\text{in}} \ll L$, and a new formula for $\psi_{2,3}$ is[11]

$$\psi_{2,3} \sim s_{2,3}\varepsilon h^{3/2} L\sqrt{L_\gamma},$$

which is only by a factor $\sim 1/\text{hL}$ smaller in comparison to Eq. (1). Thus further $\psi_{2,3}$ suppression is needed. One may use a coil of PZ-fiber. In Ref. 11, we used a numerical model for PZ-fiber, which is a generalization of model for PM-fiber.[9] According to Ref. 11, when input fiber is present, errors $\psi_{2,3}$ are anyway considerably reduced by PZ-coil, but there is one special condition of their radical suppression to an arbitrary small level, as was expected in Ref. 10. This condition has a simple form:[11]

$$\alpha L_{\text{in}} B_{\text{in}}/B \gg 1, \tag{2}$$

where α is y-mode decaying coefficient in PZ-coil. Here, input fiber plays the role of depolarizer.

As for ψ_1, PZ-coil reduces it even for minimal configuration FLI by a factor of $(\alpha L)^{1/2}$ (now it is total PNR),[11] so here corresponding rotation rate error depends as L^{-1}, contrary to $L^{-1/2}$, which followed from Eq. (1). Finally, input fiber also may be PZ, leading to additional essential suppression of ψ_1. Although input PZ-fiber is a naturally hi-bi component, it combines an input polarizer and a depolarizer for the above-described errors $\psi_{2,3}$ suppression.

In Ref. 11, we also considered PMC in input PZ-fiber and optical components axes misalignment. Although here, it is $\psi_{2,3} \neq 0$, it is still possible to greatly suppress PNR by reaching the $\psi_{2,3} \ll \psi_1$.

Thus, it is of great importance to develop PZ-fibers with different lengths (1 to 1000 m).

As a section conclusion, note that due to the condition $\psi_{2,3} \gg \psi_1$ PZ-coil in minimal configuration FLI is useful only if its dichroism is already large within the initial and final fiber sections with L_γ length, which form values of $\psi_{2,3}$. Moreover, it should come together with x-mode small bend loss. Thus, realistic PZ-coil in minimal configuration FLI does not have any advantage against PM-coil, despite a much more stable polarization through the whole PZ-coil. This is quite an impressive illustration of the difference between the interferometric (phase) processes in FLI and the fiber intensity h-parameter, so the above-declared requirement of stable polarization in fibers is necessary but not enough.

3 Refractive Index W-profile and Known PZ-Fiber Realizations Based on It

Now let us turn to refractive index W-profile with its main features and to its implementation for PZ-fiber manufacturing.

3.1 *W-Profile Definition and General Properties*

Refractive index W-profile[12] is shown in Fig. 1, along with its modification by fiber bend. It contains a core with refractive index n_1 and diameter 2ρ, depressed clad (DC) with refractive index n_2 and diameter 2τ, and pure quartz clad (refractive index n_3). For W-profile it should be $n_2 < n_3 < n_1$. Let us introduce the following parameters:

$$\Delta n_+ = n_1 - n_3,$$
$$\Delta n_- = n_3 - n_2,$$
$$\Lambda = (n_3^2 - n_2^2)/(n_1^2 - n_3^2),$$
$$\chi = \tau/\rho.$$

The convenient matched clad (MC) or compensated refractive index profile corresponds to $\Delta n_- = 0$. Thus parameters Λ and χ describe W-profile depth and width, respectively.

Further, profiles $n(x, y)$ and $n_0(x, y)$ of bent and straight fibers are related as $n(x, y) = n_0(x, y)(1+x/R)$ (R is bend radius), which is illustrated by Fig. 1 right part.

It is known that W-fiber with wide and deep enough DC may possess even a fundamental mode finite cutoff.[12] Also from Fig. 1 one may see that bending yields its own kind of "triangular" W-profile right to fiber vertical axis, which may be treated as a growth of initial W-profile depth. The latter in turn may be treated as a fundamental mode cutoff decreasing, which explains a bending loss nature. It is clear that this "triangular" W-profile also takes place in MC-fiber,[13] so here bend loss may be treated as a bending "triangular" W-fiber fundamental mode cutoff.

It is also known that birefringence yields two different W-profiles for x- and y-modes, splitting their cutoffs[14] or even setting the x-mode cutoff to be infinite.[15] This leads to a dichroism window, which, according to x- and y-modes bend loss, may be shifted to shorter wavelengths due to

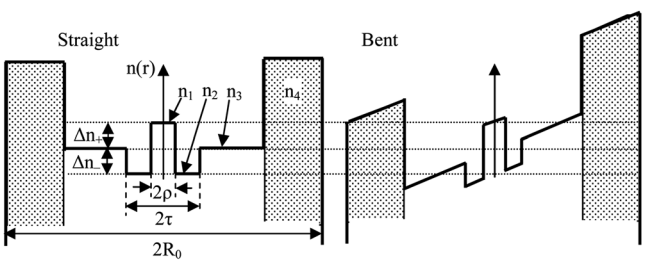

Fig. 1 Refractive index W-profiles of straight and bent fiber, 2ρ and n_1 are core diameter and refractive index, 2τ and n_2 the same for DC, n_3 is quartz cladding refractive index, $2R_0$ and n_4 are coating diameter and refractive index.

fiber bending.[14] These principles are basic for polarizing hi-bi W-fibers.

3.2 *Long Fibers (<500 m)*

First samples of long PZ-fibers for FOG coils were described in Ref. 16. These are bending type bow-tie fibers with low-aperture core, allowing the birefringence to play a significant role at the background of its small Δn. Thus a wide dichroism window is possible, which is necessary for FOG with broadband source. Here, disadvantage is a significant spreading of fundamental mode out of the core. This leads to contact with birefringence inducing stress applying parts (SAP) having a material loss.[17] Also due to this fact, it is impossible to get MFD < 10.5 μm at wavelength 1.55 μm. However, for splicing with IOC a values MFD = 6 to 8 μm are needed, otherwise, due to modes fields sizes mismatch, one gets splice loss and high-order modes excitation breaking FLI single-modal reciprocity. Here we determine MFD by fundamental mode field $E(r)$ as the value F, which maximizes the overlap integral[18]

$$I(F) = \left\{ \left(\frac{2}{F}\right) \int_0^\infty r \, \mathrm{d}\, r E(r) \exp\left[-\left(\frac{r}{F}\right)^2 \right] \right\}^2 .$$

Another long PZ-fiber sample is W-fiber with elliptical stress clad,[19] which also may be implemented for FOG sensing coil. It is based on the same principle as the fiber from Ref. 15, which also requires a low aperture core (here it is determined by $\Delta n_+ + \Delta n_- \sim 0.005$). The latter also leads to the inability of MFD varying within necessary limits and to tightly pack the fundamental mode within the core, which may result in a raised material loss within elliptical stress cladding.

Recently,[20] we described PZ-fiber Panda based on high-aperture core W-profile ($\Delta n_+ + \Delta n_- \sim 0.015$) and narrow, deep enough DC ($\chi \sim 1.7$, $\Lambda \sim 0.6$), where $2\rho = 8.3$ μm. This fiber may be associated with so called "upper" and "lower" MC-fibers with $\Delta n = \Delta n_+$ and $\Delta n = \Delta n_+ + \Delta n_-$ (Fig. 2). "Upper" fiber (and PZ-fiber from Ref. 16) advantages are: (1) wide dichroism window due to effective birefringence utilization at the background of low $\Delta n = \Delta n_+$; (2) single mode regime. Disadvantages are: (1) problem to yield MFD 6 to 8 μm; (2) loss and fundamental mode field deformation due to penetration into SAP. For "lower" fiber, due to large $\Delta n = \Delta n_+ + \Delta n_-$, one may say that situation is the reverse. The advantage of the fiber described in Ref. 20 is that it combines these two MC-fibers advantages, while leaving out their disadvantages.

Of course, as described in Ref. 20, fiber may be only treated as a prototype of polarizing W-fibers for FOG coil because its dichroism window is not wide enough.

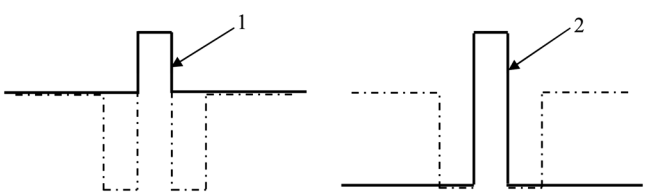

Fig. 2 "Upper" (1) and "lower" (2) MC-fibers, associated with initial W-profile (dash-dotted line).

However, its birefringence is only 3.4×10^{-4}, which is too small for such applications. Below, using this fiber, we'll test x- and y-modes bending loss mathematical models, which, in turn, will be applied to reveal that birefringence growth is extremely effective for dichroism window widening and to show that there is a wide enough class of such high-aperture core W-profiles for FOG PZ-coils with MFD at least within 6 to 10 μm.

3.3 *Short Polarizing W-Fibers (~1 m)*

As for short PZ-fibers, their most known samples are described in Refs. 14 and 15. These are W-fibers with elliptical stress clad and dichroism window relative widths of 5% (birefringence is $B = 4.7 \times 10^{-4}$) and 13% ($B = 7 \times 10^{-4}$), respectively. In Ref. 14, x- and y-modes have finite and different cutoffs, the dichroism window is in the visible spectrum region and could be shifted to smaller wavelengths by bending the fiber. In Ref. 15, the x-mode cutoff is set to be infinite in order to yield a half-infinite dichroism window (near 0.85 μm). However, the latter is also limited from above due to x-mode strong penetration into quartz cladding and thus contacting with absorbing coating. This is due to the fact that for the x-mode infinite cutoff, a low-aperture core and narrow DC are required, which cannot tightly pack the fundamental mode within the core and prevent its contact with the coating (again, it is impossible to vary MFD enough). In Ref. 19, a short PZ-fiber is also described, based on the same principle as in Ref. 15.

In Ref. 21, to our knowledge, a first Panda-type PZ-fiber is suggested with different x- and y-mode cutoffs, as in Ref. 14. In Ref. 22, we describe a practical sample of this fiber, which being 1-m length in a straight state yields a dichroism 32 dB for typical FOG broadband source, possessing a dichroism window wider than 250 nm ($B = 7.5 \times 10^{-4}$). The rest of the parameters may be taken from Ref. 22, so it is seen that this is a middle-aperture core fiber ($\Delta n_+ + \Delta n_- \sim 0.006$), and $\chi = 2.4$. X-mode spreads into quartz cladding only close to its cutoff. Below we test x- and y-mode loss mathematical models using this fiber, and then we will show that there are classes of middle- and high-aperture core W-profiles for PZ-fibers of such lengths, having MFD at least within 8 to 10 μm.

3.4 *Large-MFD PZ Fibers*

Such kinds of fibers currently are mainly microstructured ones. These fibers are under much softer bending resistance requirements or even operate without any bending (for example, so-called rod-type fibers with several mm diameter).[23] Here, air holes have a small diameter, and PZ effect is reached by SAP. Also, one should have in mind a low-aperture core fiber with two air holes from both sides of it.[3] In the latter case, SAP is also implemented to introduce the birefringence.

4 Mathematical Models

Here, we introduce two kinds of models based on a scalar wave equation (see below). One of them could be used only for straight fibers and another for both straight and bent fibers. Note that implementing them for the same problems yields the same results for each model.

4.1 *Straight Infinite Coating Fiber*

We will put for coating $n_4 = 1.54$ and $R_0 \to \infty$ (Fig. 1). Light is treated as a supermodes set.[24,25] Field $\psi_{j,l}(r,\phi)$ of supermode with azimuthal order l and number j is described by scalar wave equation:

$$\lfloor \Delta_t + k^2 n^2(r,\varphi) - (l/r)^2 \rfloor \psi_{l,j}(r,\varphi) = \beta_{l,j}^2 \psi_{l,j}(r,\varphi). \quad (3)$$

Here Δ_t is Laplace operator transverse part, k is vacuum wave number, $n(r,\phi)$ is refractive index profile, and $\beta_{j,l}$ is supermode propagation constant.

Further, in step-index W-profile Eq. (3) has analytical solutions in each region with constant refractive index.[24,25] In the coating, any supermode of interest is the outgoing cylindrical wave [Hankel function, according to Eq. (3)], carrying the energy to infinity (attenuation). In this case, a characteristic equation may be constructed using scalar boundary conditions (equalizing fields and their radial derivatives at each layer's boundary). Complex propagation constants are thus calculated, and their imaginary parts are attenuation values.

As for supermodes excitation, it is provided by input beam with the field ψ_{in}, and their further propagation through the fiber takes into account their individual attenuation coefficients:[24,25]

$$E_{l,j}(r,\varphi,z) = \sum_{l,j} A_{l,j} \psi_{l,j}(r,\varphi) \exp[-i\,\text{Re}(\beta_{l,j})z - \text{Im}(\beta_{l,j})z], \quad (4)$$

where $A_{l,j} = \int \mathrm{d}\, s \psi_{in} \psi_{l,j}^*$ with integration is carried out over the core, DC, and quartz claddings. The sign $*$ is complex conjugation. For multimode core communication W-fibers, it is better to replace this treatment by so-called power-flow equation,[26,27] where, besides this, one may take into account the modes coupling. In our case, where the fiber cores are only few-mode, it is better to start from Eq. (4), where one may introduce some simplifications. For example, considering the fundamental mode suppression, we will take a fundamental mode quasi-Gaussian beam of "lower" MC-fiber associated with the W-fiber under consideration (Fig. 2), so of all supermodes one may limit himself only by azimuthally symmetric ones ($l = 0$), i.e., Eq. (4) contains only a single sum with index j.

Moreover, it is established that at each wavelength one of the W-fiber supermodes (let us call it selected) resembles the input quasi-Gaussian beam by field distribution[24] and has a propagation constant close to this beam propagation constant. This supermode takes almost all input beam power and at the same time has minimal attenuation among the rest supermodes. Thus all supermodes calculations may be replaced by computing only the selected one. Its parameters are close to the ones of the input beam, so these latter parameters may be taken as initial approximations. For hi-bi fiber this means two selected x- and y-polarized supermodes (desired x and y modes).

The same treatment may be implemented for modal filtering estimation in few-mode core W-fiber, using the input beam in the form of first higher mode of "lower" MC-fiber (Fig. 2).

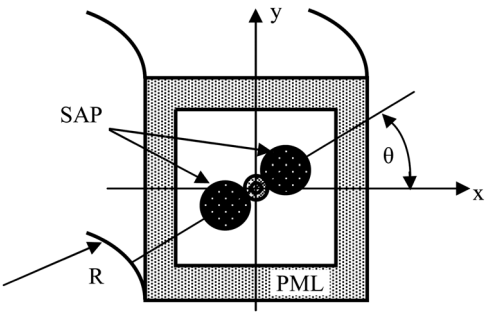

Fig. 3 W-fiber cross-section. Angle θ is SAP orientation angle in bending plane, R is bending radius.

4.2 *Frequency Domain Finite Difference Method with PML*

Here, we assume a rectangular fiber cross-section (Fig. 3) and PML is for light attenuation modeling.[28] One may use full-vectorial approach for transverse magnetic fields.[29] However, for weak guiding fibers (i.e., for all W-fibers and MC-fibers described in this paper) one may start from the scalar wave equation, similarly to the model in Sec. 4.1:

$$\left\{ \frac{\partial}{\partial x}\left[\sigma_x(x)\frac{\partial}{\partial x}\right] + \frac{\partial}{\partial y}\left[\sigma_y(y)\frac{\partial}{\partial y}\right] + k^2 n^2(x,y) \right\} E(x,y) = \beta^2 E(x,y),$$

where functions $\sigma_x(x)$ and $\sigma_y(y)$ describe PML with absorbing coefficient α and width d in the way that $\sigma_x(x) = \sigma_y(y) = 1$ outside PML, and within it they are (similar to Ref. 28)

$$\sigma_x(|x| > \rho_{\text{cl}}) = 1/\lfloor 1 + i\alpha(x - \rho_{\text{cl}})^2/d^2 \rfloor,$$
$$\sigma_y(|y| > \rho_{\text{cl}}) = 1/\lfloor 1 + i\alpha(y - \rho_{\text{cl}})^2/d^2 \rfloor.$$

Here, ρ_{cl} is quartz clad radius. Further, mesh consists of N_x and N_y steps $\Delta x = 2(d + \rho_{\text{cl}})/(N_x - 1)$ and $\Delta y = 2(d + \rho_{\text{cl}})/(N_y - 1)$ along the x and y axis:

$$x_i = -d - \rho_{\text{cl}} + (i-1)\Delta x,$$
$$y_j = -d - \rho_{\text{cl}} + (j-1)\Delta y,$$
$$(j = 1, 2 \ldots N_y).$$

According to discretization scheme from Ref. 30, one has for wave equation the following:

$$ax_i E_{i+1,j} + b_{i,j} E_{i,j} + cx_i E_{i-1,j} + ay_j E_{i,j+1} + cy_j E_{i,j-1} = \beta^2 E_{i,j},$$

where

$$ax_i = \frac{\kappa x_{i+1}}{\Delta x^2}, \qquad b_{i,j} = k^2\varepsilon_{i,j} - \frac{\kappa x_{i+1} + \kappa x_i}{\Delta x^2} - \frac{\kappa y_{j+1} + \kappa y_j}{\Delta y^2},$$

$$cx_i = \frac{\kappa x_i}{\Delta x^2}, \qquad ay_j = \frac{\kappa y_{j+1}}{\Delta y^2},$$

$$cy_j = \frac{\kappa y_j}{\Delta y^2}, \quad E_{i,j} = E(x_i, y_j), \qquad \varepsilon_{i,j} = n^2(x_i, y_j),$$

$$\kappa x_i = \frac{2\sigma x_i \sigma x_{i-1}}{\sigma x_i + \sigma x_{i-1}}, \qquad \kappa y_j = \frac{2\sigma y_j \sigma y_{j-1}}{\sigma y_j + \sigma y_{j-1}},$$

$$\sigma x_i = \sigma_x(x_i), \qquad \sigma y_j = \sigma_y(y_j).$$

Note, that a concept of quasi-Gaussian selected x- and y-supermodes is also valuable for bent fiber. First a "lower" straight MC-fiber (Fig. 2) fundamental mode field and parameters are calculated, serving then as an initial approximation for desired W-fiber selected supermode.

Exactly the same method may be used for modal filtering estimation. Here, a selected supermode is the one that is closest to the first higher-order mode of "lower" MC-fiber associated with the W-fiber under consideration (Fig. 2). However, here, instead of one selected supermode, there are two of them, which in straight fiber have fields azimuthal behavior in the forms of cos ϕ and sin ϕ. Their fields are differently deformed by fiber bending and their bend losses are not equal to each other, so modal filtering should be estimated according to the smaller one. The example of such modal filtering calculation result in W-fiber, along with its changes by bending, is presented in Ref. 31.

5 Long PZ Fiber Based on W-Profile

As was mentioned earlier in Ref. 20 a 500-m PZ W-fiber sample is described as a prototype for FOG PZ coil fiber, which was wound with a 55-mm diameter. Loss of x- and y-modes were 3 and 30 dB/km. Figure 4(a) shows experimental x- and y-modes spectral loss graphs in this sample. As was said above, the dichroism window is not wide because birefringence is only $B = 3.4 \times 10^{-4}$. We have modeled x- and y-mode bending loss by the model found in Sec. 4.2, putting SAP orientation angle to be averaged ($\theta = 45$ deg in Fig. 3), because during winding it is out of control. Results are shown on Fig. 4(b) [curves 1 and 2 are for y- and x-mode, corresponding to curves 1 and 2 on Fig. 4(a)]. After this, we introduced a $B = 8 \times 10^{-4}$, yielding for this case the dashed curves 3 and 4 for y- and x-modes loss [Fig. 4(b)], corresponding this time to a wide-enough dichroism window.

Further, in the same manner one may find a class of broadband polarizing W-profiles with different MFD at least within 6 to 10 μm. For example, in Table 1, one of just such W-profiles class parameters are listed for winding with diameter $2R = 55$ mm.

Note that for each fiber-winding diameter, $2R$, one may similarly get another W-profiles class. One general feature for all of them is the following: the larger the winding diameter, the wider the dichroism window. This is due to two reasons: (1) for larger radii of fiber bend a lower values of Δn_+ are needed, so the birefringence role in x- and y-modes loss curves splitting becomes more significant; (2) bend by itself leads to dichroism window reduction. Thus in a straight fiber it is easy to get a dichroism window over 300 nm. As for modal filtering, according to the model in Sec. 4.1, it should be very effective in all cases.

6 Short Polarizing W-Fibers (1 to 10 m)

For another test of described above mathematical models, we used x- and y-modes spectral loss curves from Ref. 22 [Fig. 5(a)]. Here, x-mode loss (curve 2) sharp growth near 1.7 μm is due to instrumental spectrum analyzer limitations (not to cutoff). Calculation by the model in Sec. 4.1 yields good agreement with the experiment for straight fiber x- and y-mode loss [1 and 2 on Fig. 5(a)]. For x-mode bend loss we used the model in Sec. 4.2 with SAP, having reduced refractive index. For this case, Fig. 5(b) shows several loss graphs. Graphs 1 and 2 are y- and x-mode loss in a straight fiber, thick lines 3 and 4 are the same in bent fiber, averaged within SAP orientation angle θ region 0 ± 20 deg (see Fig. 3), and dash-dotted lines 5 and 6 are the same in bent fiber at fixed $\theta = 90$ deg. Thus theoretical curves 1 to 4 on Fig. 5(b) correspond to experimental curves 1 to 4 on Fig. 5(a). A good agreement between theory and experiment is seen except resonance on curves 1 and 3 at wavelength 1.425 μm [Fig. 5(b)]. Probably this is due to W-profile parameter changes along the fiber, smoothing out this resonance on Fig. 5(a). Another dip at 1.45 μm on Fig. 5(b) is due to SAP, according to calculations. On Fig. 5(a) it has a lower depth (curve 1), and this again could be due to its smoothing by longitudinal W-profile changes. As for x-mode bend loss averaging

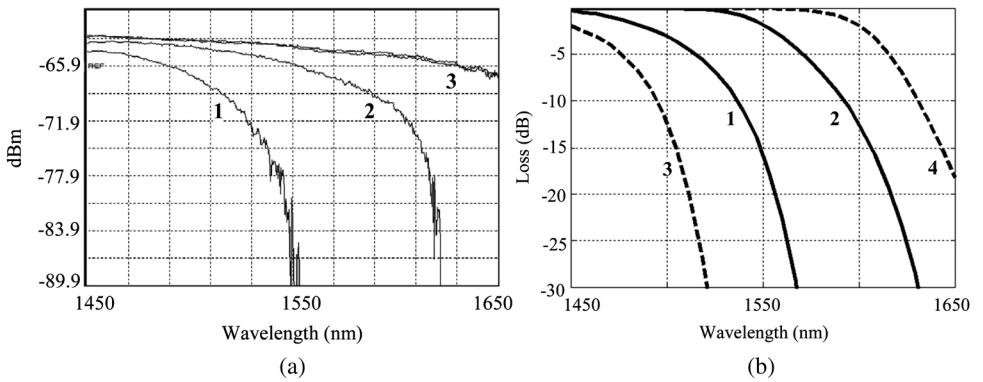

Fig. 4 Y- and x-modes spectral loss in PZ-fiber (1 and 2) and light spectra (3), exciting x- and y-modes (a), and theoretical x- and y-mode attenuation spectra for W-fiber Panda wound on 55-mm diameter carcass (b). Curves 1 and 2 on (b) are for y- and x-mode at birefringence $B = 3.4 \times 10^{-4}$, curves 3 and 4 on (b) are the same at $B = 8.0 \times 10^{-4}$.

Table 1 Refractive index W-profiles parameters for FOG coil PZ-fiber with different MFD, wound with 55-mm diameter (one example of W-profiles class).

W-profile parameters	MFD = 6 μm	MFD = 7 μm	MFD = 8 μm	MFD = 9 μm	MFD = 10 μm
Δn_+	0.0086	0.0067	0.0053	0.0043	0.0038
Δn_-	0.009	0.009	0.009	0.009	0.009
2ρ (μm)	5.8	7.1	8.9	10.7	12.2
χ	1.7	1.7	1.7	1.6	1.5
High order mode cutoff (μm)	0.98	1.05	1.16	1.25	1.34

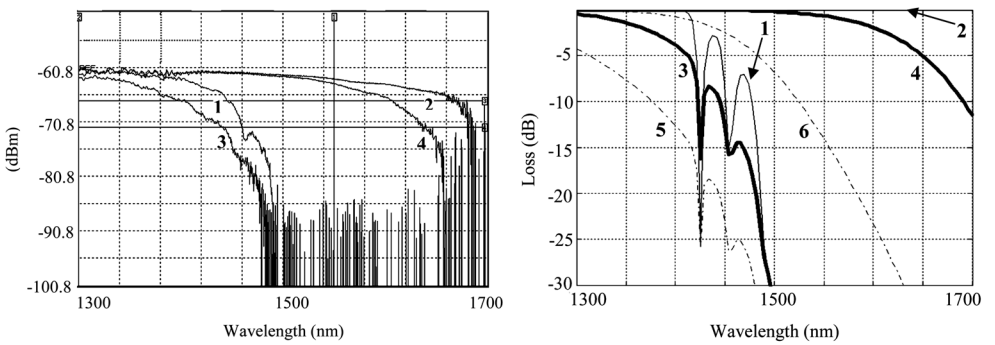

Fig. 5 (a) Experimental graphs of W-polarizer spectral loss, 1 and 2 for y- and x-mode in straight fiber, 3 and 4 in bent fiber (three turns with 60-mm diameter). (b) Curves 1 and 2 are y- and x-mode loss in straight fiber, thick curves 3 and 4 are the same in bent fiber at SAP angle θ averaging within $\theta = \pm 20$ deg, curves 5 and 6 (dash-dot) are the same in bent fiber at $\theta = 90$ deg.

within $\theta = 0 \pm 20$ deg, this corresponds to the fact that this loss in experiment was dependent on fiber installation in table.[22]

Strictly speaking, here, the dichroism window in bent fiber has zero width and is situated near 1.5 μm. For 0.1-dB x-mode bending loss at 1.55 μm it should be $\theta = 0$ deg. On the contrary, at $\theta = 90$ deg the dichroism window is absent [curves 5 and 6 on Fig. 5(b)], or even in some sense one might say that it has a negative width. At the same time, setting the SAP refractive index equal to the quartz cladding index, one will get loss close to the latter case of $\theta = 90$ deg. Thus SAP with lower refractive index not only introduces anisotropy but also significantly prevents dichroism window bending reduction.

Consider now the birefringence $B = 0.001$. It is achievable in Panda fibers, at least with 125-μm diameter, which is considered by us for short PZ-fibers. For example, Ref. 32 reports about $B = 1.15 \times 10^{-3}$ in bow-tie fiber, which are only slightly better in this sense than Panda fiber. In Table 2, parameters are listed for two W-profiles, yielding almost the same dichroism windows for 60-mm bending diameter (in straight fibers dichroism windows are different). The first W-profile is a small modification of the profile from Ref. 22 with a slightly raised Δn_+, the second W-profile is high-aperture core, similar to the above-considered (Sec. 5) W-profile for FOG coil PZ-fiber. Calculations for Table 2 also took into account SAP influence. Here, when angle θ averaging of x-mode bending loss within the limits $\theta = \pm 45$ deg we have got 0.1 dB, a necessary value plus many more soft requirements to fiber installation. Note that at bending diameters $2R > 70$ mm fiber may be installed arbitrarily.

Thus, none of the W-profiles by themselves provide the wide-band dichroism even with high birefringence. SAP with reduced refractive index is also necessary for x-mode bending loss decreasing.

Further, in Table 3, another two possible W-profiles are presented for MFD = 8 μm. Note that the second one is

Table 2 Example of refractive index W-profiles parameters for 1-m PZ-fiber with MFD = 10 μm.

Parameter	Profile 1	Profile 2
Δn_+	0.0029	0.0024
Δn_-	0.0033	0.009
2ρ	9.5 μm	12.0 μm
χ	2.4	1.6
x- and y-modes cutoff difference	486 nm	457 nm
Dichroism window (straight fiber)	>300 nm	300 nm

Table 3 Example of refractive index W-profiles parameters for 1-m PZ-fiber with MFD = 8 μm.

Parameter	Profile 1	Profile 2
Δn_+	0.0045	0.0038
Δn_-	0.0045	0.009
2ρ (μm)	7.3	9.0
χ	2.3	1.7

again a high-aperture-core narrow-DC W-profile. Thus a class of W-profiles is possible for each MFD, at least within 8 to 11 μm. This widens a region of possible MFD of PZ-fibers, known from literature. For MFD = 6 to 8 μm one should consider another W-profiles class; these will, of course, be high-aperture-core profiles, including a very high-aperture core available by the SPCVD method.[33]

In accordance with the above, we also suggest PZ-fiber construction with the cross-section shown in Fig. 6. Here, initially a W-profile in circular preform is manufactured for 250-μm diameter fiber. Then the preform is polished from two sides but between the rods and fiber boundary a thick enough quartz layer is left. Drawn fiber is wound on one of the flat boundaries to maintain the SAP orientation, which is most desirable for dichroism window. Such a fiber could be wound with a 30-mm diameter.

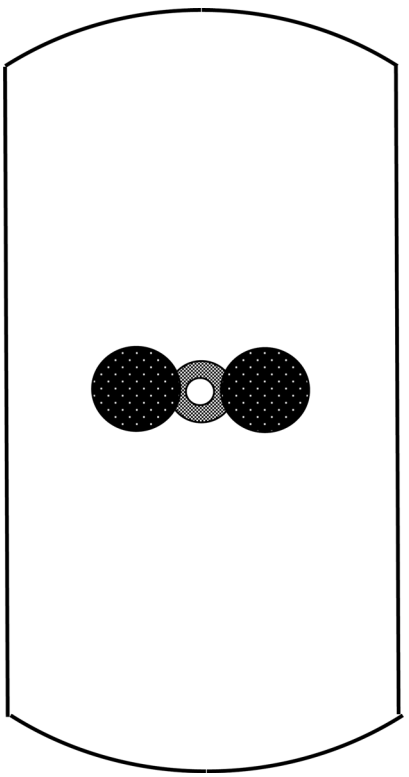

Fig. 6 Flat W-fiber Panda.

7 Large-MFD W-Fibers

These are not of interest for FOG, but they are useful for high-power fiber lasers. The spectral range here is near 1.06 μm with standard MFD = 6 to 7 μm. In MC SM fiber, which may be bent with a 60-mm diameter, according to calculations maximal MFD = 11.2 μm($\Delta n = 0.0023$, $2\rho = 10.1$ μm). For fibers with large MFD, it is better to determine this parameter by effective mode area A of two-dimensional mode field distribution $E(x, y)$:[34]

$$\mathrm{MFD} = 2\sqrt{\frac{A}{\pi}}, \qquad A = \frac{[\int_{-\infty}^{+\infty}\int_{-\infty}^{+\infty} \mathrm{d}x\mathrm{d}y|E(x,y)|^2]^2}{\int_{-\infty}^{+\infty}\int_{-\infty}^{+\infty} \mathrm{d}x\mathrm{d}y|E(x,y)|^4}.$$

7.1 *Middle-Aperture-Core W-Fiber*

Applying the middle-aperture-core W-profile one may raise MFD at least to 12.4 μm. In Table 4, parameters are listed for realized Panda fiber. This 200-m fiber was wound with 160-mm diameter and h-parameter was 10^{-8} 1/m, which is obviously due to dichroism. Calculated value for the first high-order mode loss is >15 dB/m (straight fiber), and fundamental mode loss is <0.2 dB for one 60-mm diameter turn. Indeed, far-field scanning revealed a good SM light beam after the straight 1-m fiber. Here, similar to the dichroism window, it is possible to introduce the SM window oriented on high-order mode 10 dB attenuation.

For such types of W-profiles it is probably the maximum MFD that could be reached for the combination of bend resistance and SM regime in a straight fiber. Using such types of W-fibers for larger MFD could only be done through fundamental and high-order modes bend losses difference (as in Ref. 35 for convenient MC low-aperture fiber). We applied the model in Sec. 4.2 to bent middle-aperture-core W-fibers of the same kind as in Table 4 but with lower Δn_+ and larger 2ρ for MFD ~ 30 μm. Also a small $\chi \sim 1.3$ to 1.4 was chosen for high-order modes filtering out. According to calculations, higher-order mode loss is only three to four times larger than that of the fundamental mode.

7.2 *Straight Short Modal and Polarization W-Filters*

Fiber bending reduces its SM-window similar to the dichroism window in PZ-fibers. Thus, it is natural to ask for straight modal filters with lengths 0.1 to 0.5 m. In this case, it is also possible to use refractive index W-profile. We will start from a profile with pure silica core and DC with refractive indices regulated by SAP-introducing birefringence B[36,37] Thus one

Table 4 Refractive index W-profile parameters for fiber with MFD = 12 μm at 1.06 μm.

Parameter	Value
Δn_+	0.001
Δn_-	0.004
2ρ (μm)	15.4
χ	2.0

Table 5 Example of refractive index W-profiles parameters for fiber modal and polarization filters samples with MFD = 32 and 73 μm at 1.06 μm.

Parameter	MFD = 32 μm	MFD = 73 μm
$B(=2\Delta n_+)$	$4.2 - 5.5 \times 10^{-4}$	$0.5 - 0.7 \times 10^{-4}$
Δn_-	0.001	2.5×10^{-4}
2ρ (μm)	40	90
$\chi = \tau/\rho$	1.2	1.1

has $\Delta n_+ = B/2$. Such a way to regulate core index is much more accurate than with core doping. Here, the refractive index for y-mode is lower than the quartz index, so this is also a PZ-fiber. In this case, DC should be narrow for high-modes effective attenuation due to effective penetration into the quartz cladding. The latter will also lead to high-order x-mode exciting with small amplitude by the input of a high-order mode of a multimode fiber (small fields overlap integral). This will give an additional 4 to 5 dB for filtering efficiency, which is essential especially for 0.1-m filters. Also note that due to a narrow DC, fundamental x-mode cutoff frequently is infinite, similar to the PZ-fiber from Ref. 14.

In Table 5, the parameters of W-profile are listed for such filters with 0.1-m length and MFD near 32 and 73 μm. It is clear that in both cases, the core is low aperture due to the fact that by making the DC by fluorine doping it is possible to regulate this accurately enough by the value Δn_-. W-profile parameters in Table 5 are only the particular variants for each MFD. It is also possible to construct similar profiles for all MFD values from 30 to 70 μm. Here, DC determines the modes' cutoffs and concentrates the light in the core, reducing the SAP influence on it, i.e., improving the beam quality.

It should be specially noted that birefringence may be widely varied (~30%, see Table 5). This is good for operation under strong heating. However, such short fibers could be cooled. Besides all of this, one may use additional scattering/absorbing inserts in fiber cross-sections (layers and rods).[37] Earlier,[22] for standard MFD W-fiber we introduced an absorbing/scattering layer into cladding and it yielded an increase of y-mode loss in 50-mm W-fiber section from 1 to 3 dB to 15 dB (see Ref. 22 for details).

8 Conclusion

We considered PZ-fibers based on refractive index W-profile. For FOG sensing coils (long fibers) high-aperture-core W-fibers are possible. For PZ-fibers with smaller lengths (1 to 10 m), which could be used as input fiber in fiber loop interferometer (FLI), W-profiles with high- and middle-aperture-core are suitable. For this second case, we have shown that necessary bend resistance may be achieved only with the help of the reduced refractive index of SAP, which significantly prevent the dichroism window narrowing due to bending. Finally, for large MFD PZ-fibers for high-power fiber lasers, W-profiles are possible with middle- and low-aperture core (the latter for very large MFD).

References

1. Y. Yamamoto and T. Kimura, "Coherent optical fiber transmission systems," *IEEE J. Quantum Electron.* **17**(6), 919–935 (1981).
2. R. Ulrich, "Fiber-optic rotation sensing with low drift," *Opt. Lett.* **5**(5), 173–175 (1980).
3. M.-J. Li et al., "Fiber designs for higher power lasers," *Proc. SPIE* **6469**, 64690H (2007).
4. E. Kintner, "Polarization control in optical-fiber gyroscopes," *Opt. Lett.* **6**(3), 154–156 (1981).
5. K. Burns et al., "Fiber-optic gyroscopes with broad-band sources," *J. Lightwave Technol.* **1**(1), 98–105 (1983).
6. A. Kurbatov, "Report on fiber gyroscope development," (in Russian) *Arzamas, "Impulse"* (1984).
7. W. K. Burns and R. P. Moeller, "Polarizer requirements for fiber gyroscopes with high-birefringence fiber and broad-band sources," *J. Lightwave Technol.* **2**(4), 430–435 (1984).
8. S. M. Kozel et al., "Effect of random inhomogeneities in a fiber light-guide on the null shift in a ring interferometer," *Opt. Spectrosc.* **61**(6), 814–816 (1986).
9. G. B. Malykin et al., "Mathematical simulation of random coupling between polarization modes in single-mode fiber waveguides: I. evolution of the degree of polarization of nonmonochromatic radiation traveling in a fiber waveguide," *Opt. Spectrosc.* **83**(5), 780–789 (1997).
10. E. Jones and J. W. Parker, "Bias reduction by polarization dispersion in the fiber-optic gyroscope," *Electron. Lett.* **22**(1), 54–56 (1986).
11. A. M. Kurbatov and R. A. Kurbatov, "Suppression of polarization errors in fiber-ring interferometer by polarizing fibers," *Tech. Phys. Lett.* **37**(5), 397–400 (2011).
12. S. Kawakami and S. Nishida, "Characteristics of a doubly clad optical fiber with a low-index inner cladding," *IEEE J. Quantum Electron.* **10**(12), 879–887 (1974).
13. H. Vendeltorp-Pommer and J. Hedegaard Povlsen, "Bending loss and field distribution in a bent fibre calculated with a beam propagating method," *Opt. Commun.* **75**(1), 25–28 (1990).
14. J. R. Simpson et al., "A single-polarization fiber," *J. Lightwave Technol.* **1**(2), 370–373 (1983).
15. M. Messerly et al., "A broad-band single polarization optical fiber," *J. Lightwave Technol.* **9**(7), 817–820 (1991).
16. M. Varnham et al., "Single-polarisation operation of highly birefringent bow-tie optical fibers," *Electron. Lett.* **19**(7), 246–247 (1983).
17. K. Tajima and Y. J. Sasaki, "Transmission loss of a 125-μm diameter PANDA fiber with circular stress-applying parts," *J. Lightwave Technol.* **7**(4), 674–679 (1989).
18. D. Marcuse, "Gaussian approximation of the fundamental modes of graded-index fibers," *J. Opt. Soc. Am.* **68**(1), 103–109 (1978).
19. C. H. Wang et al., "Highly polarizing single-mode optical fiber for sensing applications," *Proc. SPIE* **7503**, 75034F (2009).
20. A. M. Kurbatov and R. A. Kurbatov, "New optical W-fiber Panda for fiber optic gyroscope sensitive coil," *Tech. Phys. Lett.* **36**(9), 789–791 (2010).
21. A. M. Kurbatov, "Single mode single polarization fiber for polarization modal filter," R.U. Patent No. 2040493 (1990).
22. A. M. Kurbatov and R. A. Kurbatov, "Fiber polarizer based on W-light-guide Panda," *Tech. Phys. Lett.* **37**(7), 626–629 (2011).
23. O. Schmidt et al."Single-polarization ultra-large-mode-area Yb-doped photonic crystal fiber," *Opt. Express* **16**(6), 3918–3923 (2008).
24. P. L. Francois and C. Vassallo, "Finite cladding effects in W fibers: a new interpretation of leaky modes," *Appl. Opt.* **22** (19), 3109–3120 (1983).
25. J. A. Besley and J. D. Love, "Supermode analysis of fibre transmission," *IEE Proc. Optoelectron.* **144**(6), 411–419 (1997).
26. A. Simovic et al., "Influence of depth of intermediate layer on optical power distribution in W-type optical fibers," *Appl. Opt.* **51**(20), 4896–4901 (2012).
27. S. Savovic et al., "Explicit finite difference solution of the power flow equation in W-type optical fibers," *Opt. Laser Technol.* **44**(6), 1786–1790 (2012).
28. Y. Tsuchida et al., "Design and characterization of single-mode holey fibers with low bending losses," *Opt. Express* **13**(12), 4770–4779 (2005).
29. V. Dangui et al., "A fast and accurate numerical tool to model the modal properties of photonic-bandgap fibers," *Opt. Express* **14**(7), 2979–2993 (2006).
30. A. N. Tikhonov and A. A. Samarskii, *Equations of mathematical physics* (in Russian), Nauka, Moscow (1977).
31. A. M. Kurbatov and R. A. Kurbatov, "Methods of improving the accuracy of fiber-optic gyros," *Gyroscopy Nav.* **3**(2), 132–143 (2012).
32. A. Ourmazd et al., "Thermal properties of highly birefringent optical fibers and preforms," *Appl. Opt.* **22**(15), 2374–2379 (1983).
33. A. L. Tomashuk and K. M. Golant, "Radiation-resistant and radiation-sensitive fibers," *Proc. SPIE* **4083**, 188–201 (2000).
34. N. A. Mortensen, "Effective area of photonic crystal fiber," *Opt. Express* **10**(7), 341–348 (2002).

35. Y. Jeong et al., "Ytterbium-doped large-core fiber laser with 1.36 kW continuous-wave output power," *Opt. Express* **12**(25), 6088–6092 (2004).
36. A. M. Kurbatov and R. A. Kurbatov, "Polarizing single mode fiber," RU Patent No. 2250482 (2003).
37. A. M. Kurbatov and R. A. Kurbatov, "Way of manufacturing of polarizing W-fiber with fundamental mode spot large diameter," RU Patent No. 2269147 (2004).

Alexander M. Kurbatov graduated from the radiophysical department of Gorky (now Nizhny Novgorod) State University, Russian Federation, in 1977. Since 1980, his research interests have been related to fiber optic gyroscopes and fiber optic components for them.

Roman A. Kurbatov graduated from the radiophysical department of Nizhny Novgorod State University, Russian Federation, in 1998. His research interests are related to the optical waveguides theory and fiber optic gyroscope principles.